IFSO®

Check for updates

Gastric Bypass with Different Biliopancreatic Limb Lengths Results in Similar Post-absorptive Metabolomics Profiles

Ivana Jarak[1] · Sofia S. Pereira[2,3,4,5] · Rui A. Carvalho[6] · Pedro F. Oliveira[1,4,7] · Marco G. Alves[1,7] · Marta Guimarães[2,3,8] · Nicolai J. Wewer Albrechtsen[9,10,11] · Jens J. Holst[9,10] · Mário Nora[8] · Mariana P. Monteiro[2,3]

Abstract

Background/Aim Roux-en-Y gastric bypass (RYGB) with a long biliopancreatic limb (BPL) was demonstrated to further improve type 2 diabetes (T2D) outcomes. Whether benefits occur at the cost of a negative impact on nutrient absorption is a matter of debate. Our aim was to evaluate the impact of RYGB BPL length on short-term nutrient absorption.

Methods Subjects ($N = 20$) submitted to RYGB with a 2 m BPL ($n = 11$) or standard BPL (60–100 cm) ($n = 9$) 4.2 ± 0.4 years earlier underwent a mixed meal tolerance test. Plasma metabolites were analyzed at baseline and after meal by nuclear magnetic resonance (NMR) spectroscopy. Spectra were subject to multivariate analysis (MVA). Partial least square discriminant analysis (PLS-DA) was used to identify metabolites responsible for group discrimination.

Results Principal component analysis and PLS-DA showed a clear separation between plasma metabolites before and 30 min after meal intake in both groups. The metabolites responsible for differences between time points were glucose and branched-chain amino acids. A complete overlap in metabolite species and concentrations was observed at 0 and 30 min time points for both groups, while acetate levels 120 min after the meal intake were significantly higher in subjects submitted to RYGB with a 2-m-long BPL as compared to the group submitted to the standard RYGB procedure.

Conclusions Post-prandial plasma metabolomics profiles suggest that a 2-m-long BLP RYGB does not have a negative impact on acute metabolite absorption. RYGB BPL length seems to influence post-prandial acetate levels, which could contribute to the additional positive metabolic outcomes.

Keywords Bariatric surgery · Gastric bypass · Metabolomics profiles

Introduction

Roux-en-Y gastric bypass (RYGB) is one of the most frequently performed bariatric surgeries [1, 2]. RYGB surgery was designed as a combination of a restrictive procedure, derived from reduction of the stomach volume by creation of a small gastric pouch and a moderate malabsorptive procedure derived from partial exclusion of the small intestine, comprising the

✉ Mariana P. Monteiro
mpmonteiro@icbas.up.pt

Ivana Jarak
jarak.ivana@gmail.com

Sofia S. Pereira
spereira.bq@gmail.com

Rui A. Carvalho
carvalho@bioq.uc.pt

Pedro F. Oliveira
pfobox@gmail.com

Marco G. Alves
alvesmarc@gmail.com

Marta Guimarães
martafilomenaguimaraes@gmail.com

Nicolai J. Wewer Albrechtsen
nicolai.albrechtsen@sund.ku.dk

Jens J. Holst
jjholst@sund.ku.dk

Mário Nora
mario.nora@chedv.min-saude.pt

Extended author information available on the last page of the article

duodenum and proximal jejunum from the gastro-intestinal transit [3, 4]. Most patients submitted to RYGB experience a substantial and sustained weight loss, as well as a significant improvement or resolution of obesity-associated comorbidities, which is particularly prominent for type 2 diabetes (T2D) [5–9]. The anti-diabetic effect of RYGB has been attributed not only to caloric restriction, but mostly to modified endocrine dynamics derived from the anatomical rearrangement of the gastro-intestinal tract, which promotes the exclusion of the proximal intestine while allowing the early arrival of nutrients to the distal ileum [10–12].

More recently several technical variants to the RYGB procedure initially described have been introduced, most of which involve modifications of either the alimentary or biliopancreatic intestinal limb lengths, devised with the ultimate aim of potentiating either weight loss and/or the anti-diabetic outcomes [4, 13–16]. Among these, a RYGB with a 2-m-long biliopancreatic limb (BPL) was demonstrated to result in a higher rate of disease remission, a lower percentage of disease relapse, and a reduced need for anti-diabetic drugs to achieve optimal glycemic control in those patients with persistent T2D disease [17]. A distinctive hormone profile favoring improved metabolic profiles with increased post-prandial glucagon-like peptide-1 and neurotensin responses in individuals who submitted to the 2-m-long BPL RYGB procedure as compared to the standard technique was also observed [18].

There is no clinical evidence that 2-m-long BPL RYGB results in a higher risk of nutrient deficiencies. However, since nutrients are differentially absorbed over the small intestine [19, 20], the exclusion of a longer intestinal length could increase the malabsorption rate.

The putative contribution of the surgical modification on metabolite absorption is still a matter of debate and so the aim of this study was to evaluate the impact of RYGB BPL length on metabolic fingerprint using an ^{1}H-NMR metabolomics approach.

Materials and Methods

Participants

Study participants were recruited among the post-bariatric surgery cohort under routine follow-up in a single public bariatric center. The study protocol including permission to access to the patient register were approved by Institution Ethical Review Board. All procedures performed in studies involving human participants were in accordance with the ethical standards of the institutional and/or national research committee and with the 1964 Helsinki declaration and its later amendments or comparable ethical standards. Informed consent was obtained from all individual participants included in the study.

Study Design

Subjects that accepted to participate and met the eligibility criteria of having been previously submitted to a RYGB procedure either with a standard or 2-m-long BPL, while being weight stable for at least the previous 6 months were included in the study. Exclusion criteria included ongoing pregnancy, fasting plasma glucose > 7.0 mmol/L, past medical history of T2D, glucose intolerance, or dumping syndrome.

Subjects were submitted to a standard RYGB procedure (n = 9) or to a RYGB variant with a 2-m-long BPL (n = 11), 3.8 ± 2.1 or 4.4 ± 1.7 years before study enrolment, respectively.

All surgeries were performed at a single hospital institution, using a standard laparoscopic RYGB technique by the same team of bariatric surgeons only differing in the BPL length: 87.8 ± 20.5 cm (minimum 60 cm and maximum 100 cm) for the standard procedure and 200 cm for the long BPL RYGB variant, both with a constant 120-cm alimentary limb, as previously described [18]. Allocation to the surgical technique was performed according to the surgeon preference (MN, MG) based on patients' clinical and anatomical features.

After a 12-h overnight fast, subjects underwent a mixed meal tolerance test (MMTT), with a commercially available standardized liquid meal [Fresubin Energy Drink, 200 mL, 300 kcal (50E% carbohydrate, 15E% protein, and 35E% fat); Fresenius Kabi Deutschland, Bad Homburg, Germany] ingested over a maximum period of 15 min. During the MMTT, participants were kept in a seated reclined position, while venous blood was sampled before and again at 30 and 120 min after the meal ingestion. Venous blood was collected from a catheter placed in an antebrachial vein into chilled EDTA tubes (S-Monovette® 7.5 mL, K2 EDTA Gel, 1.6 mg/mL, Sarstedt), centrifuged (Rotina 380R, Hettich, 2500×g), and plasma was stored frozen in cryotubes (− 20 °C) until analyzed.

Total Plasma Amino Acid Measurement

Total L-amino acid levels were quantified, as previously described [21].

NMR Spectroscopy

Plasma samples were thawed, homogenized using vortex, and centrifuged (9200 rpm, 5 min). To 180 μL of plasma, a 45 μL fumarate solution in D_2O (2 mM, pH 7) was added. After homogenization and centrifugation (9200 rpm, 5 min), 200 μL of each sample was transferred to 3-mm NMR tube and analyzed. NMR spectra were acquired on a Varian Inova 600 MHz (14.1 T) spectrometer equipped with a 3-mm QXI probe with a z-gradient. ^{1}H cpmg (Carr-Purcell-Meiboom-Gill spin-echo pulse sequence) experiments with water pre-saturation were acquired at 298 K, using a 9.6 kHz spectral width, 90° pulse angle, 4-s

relaxation delay with 2.5 s of water pre-saturation, and 2.5 s acquisition time. Typically, for cpmg spectra, 128 scans were collected, with 8 dummy scans, total spin-spin relaxation delay of 0.75 ms, and 374 loops. Water saturation frequencies were optimized for each sample. Spectra were processed by applying exponential line broadening (lb 0.3 Hz), zero-filling to 64 k, and manual phasing and baseline correction. Chemical shifts were internally referenced to alanine doublet at 1.48 ppm. Metabolite assignment was based on comparison with previously published data and reference spectra available in public databases such as HMBD [22]. Additionally, 2D homonuclear TOCSY spectra were recorded to help spectral assignment [23].

Statistical Analysis

Data matrix for multivariate analysis was created in Amix-viewer (version 4.0.1, BrukerBiospin, Rheinstetten) using all intensity values in the 0.75–5.3 ppm region with the exclusion of water and fumarate regions, as well as the regions without signals. Processed spectra were aligned by using icoshift algorithm [24] to minimize the peak shift variations and normalized by probabilistic quotient to account for matrix dilution effects [25]. Multivariate analysis was performed in Simca 14 (Umetrics, Umea, Sweden) on a unit-variance scaled data matrices. Initial data structure was evaluated by principal component analysis (PCA), followed by partial least square discriminant analysis (PLS-DA) to identify metabolite contribution to class separation. Loadings of pair-wise comparison PLS-DA models were calculated by multiplying the variable weights (w) with the respective standard deviations and were color-coded according to the size of variable importance on projection (VIP) values. VIP > 1 were considered as relevant to group separation. Default 7-fold cross-validation and permutation test [26] were used to validate the quality of the models by assessing the values of the observed variation (R^2) and predictive potential (Q^2) of PLS-DA models. Additionally, well-resolved peaks of metabolites identified by PLS-DA loadings were integrated (Amix-viewer, version 4.0.1, BrukerBiospin, Rheinstetten) and normalized by probabilistic quotient. Normalized areas were analyzed by repeated measures two-way ANOVA (with Geisser-Greenhouse correction for the assumption of sphericity) followed by Tukey's post hoc tests (Graph-Pad Prism 6 for Windows, GraphPad Software, La Jolla, CA, USA). Metabolite levels between the two groups (standard and long BPL) were compared using two-tailed t test. For the total amino acid evaluation, the total area under the curve (tAUC) was calculated using the trapezoidal rule and incremental area under the curve (iAUC) was calculated subtracting the basal values to the tAUC. For normally distributed variables, the two groups were compared using unpaired two-tailed t test. Variables that did not follow a normal distribution were compared using the Mann-Whitney test (Graph-Pad Prism 6).

Results

There were no significant differences in the anthropometric and metabolic features between the two patient groups both at pre-operative time or post-operatively at the time of the MMTT (Table 1).

Table 1 Anthropometric and metabolic characteristics of subjects previously submitted to standard RYGB ($n = 9$) or long BPL RYGB ($n = 11$) both at the time of the surgery (preoperative) and at the time of the mixed meal (postoperative)

	Standard BPL	Long BPL	p value
N (% of total)	9 (45%)	11 (55%)	-
Gender (male/female)	1/8 (11%/89%)	1/10 (9%/91%)	0.88
Caucasians	9 (100%)	11 (100%)	
Age at time of surgery (years)	38 ± 3	43 ± 2	0.17
Pre-operative body weight (kg)	111 ± 15	105 ± 4	0.34
Pre-operative BMI (kg/m^2)	41.8 ± 1.1	40.6 ± 0.9	0.40
Post-operative body weight (kg)	74.8 ± 8.5	67.5 ± 8.3	0.07
Post-operative BMI (kg/m^2)	28.1 ± 2.3	26.2 ± 2.8	0.12
EBMIL (%)	81.7 ± 14.3	93.1 ± 18.0	0.14
TWL (%)	32.5 ± 2.0	35.3 ± 2.0	0.38
Post-operative fasting glucose (mmol/L)	5.1 ± 0.3	4.7 ± 0.6	0.18
Post-operative fasting insulin (pmol/L)	46.0 ± 18.4	41.0 ± 15.7	0.52
Post-operative Hb1Ac	5.4 ± 0.1	5.2 ± 0.1	0.42
Post-operative HOMA-IR	1.4 ± 0.6	1.2 ± 0.4	0.41
Post-operative HOMA-β (%)	110.5 ± 25.6	115.5 ± 73.2	0.85
Time after surgery (years)	3.8 ± 2.1	4.4 ± 1.7	0.51

BMI body mass index, *BPL* biliopancreatic limb, *EBMIL* excess BMI loss, *Hb1Ac* Hemoglobin A1c, *HOMA-IR* homeostasis model assessment for insulin resistance, *HOMA-β* homeostasis model assessment for β cell function, *TWL* total weight loss

Plasma samples collected during MMTT were analyzed by ¹H-NMR spectroscopy. Spectra were collected for three chosen time points corresponding to the fasting state (0 min), postprandial peak glucose after oral mixed meal ingestion (30 min), and time point of glucose clearance with resumption to steady state (120 min). Typical ¹H cpmg spectra of all three time points are presented in Fig. 1.

Due to the chosen cpmg experimental parameters, almost all the broad peaks belonging to the lipids and proteins were suppressed. However, the signals of some of the small metabolites were suppressed as well and it was possible to observe only the most abundant metabolites [27]. Various endogenous metabolites were detected in fasting blood plasma (time 0). Although the most predominant metabolite was glucose, other prominent multiplets were ascribed to amino acids such as alanine, valine, and glycine. Apart from amino acids, metabolites from the class of organic acids (acetate, acetoacetate) were also detected. The list of all identified metabolites is presented in Table 2.

Visual inspection of spectra belonging to different time points indicates transitory increase in glucose and branch-chained amino acids at 30 min. To gain more insight into possible postprandial metabolic differences between standard and long BPL RYGB, multivariate analysis was applied to the NMR spectra. The unsupervised principal component analysis was applied to normalized spectra to reveal internal data structure, and the PCA scatterplot shows a clear clustering trends and separation of all observed time points in both standard and long BPL (Fig. 2a). However, high degree of overlap was observed between standard and long BPL at all time points suggesting similarity of metabolome. To maximize the group separation, the supervised partial least square discriminant analysis was performed confirming differences observed in PCA (Fig. 2b).

Pair-wise comparisons between different time points for each RYGB procedure as well as for different BPL lengths within each time point were performed to elucidate the time course of metabolic changes and the influence of BPL length on blood plasma metabolome. In the case of comparison of standard and long BPL at individual time points, complete overlap was observed in PCA models between the two groups at all time points (data not shown) as was previously observed for comparison of all groups (Fig. 2). PCA scores and PLS-DA loading plots of different time points for standard BPL provided information about time-dependent changes in small metabolite content (Fig. 3).

A complete overlap in metabolite species and concentrations was observed at 0 and 30 min time points for both groups. Acetate levels at 120 min after the meal intake were significantly higher in subjects submitted to the long BPL RYGB compared to the group submitted to the standard RYGB procedure (Fig. 4).

Post-prandial glucose levels in both BPL groups reached peak values after 30 min and were statistically different from fasting (0 min) and terminal (120 min) glucose levels which is in agreement with previously observed results of biochemical measurements [18]. Similar to the trend observed for glucose are the levels of some amino acids, namely branched-chain amino acids (Val, Leu, Ile) which were also statistically higher at 30 min from other measured time points. However, some other amino acids like Gly and Gln demonstrate tendency of decreasing below fasting levels within the time frame of this experiment (120 min). On the contrary, Pro levels continually rise above the fasting levels during 120 min. Levels of some measured amino acids did not change during the experiment (Ser and Ala). Although some other amino acids were identified in the NMR spectra and were potentially interesting for analysis (VIP > 1), the signals were either too low (low signal to noise) or the multiplets

Fig. 1 Typical ¹H-NMR cpmg spectrum of blood plasma for three different time points (0, 30, and 120 min). Signals of some major metabolites are indicated: Ace acetoacetate, Ac acetate, Ala alanine, EDTA ethylenediaminetetraacetic acid, Glc glucose, Gln glutamine, Lac lactate, Mal malic acid, NAG N-acetyl glycoprotein, Val valine
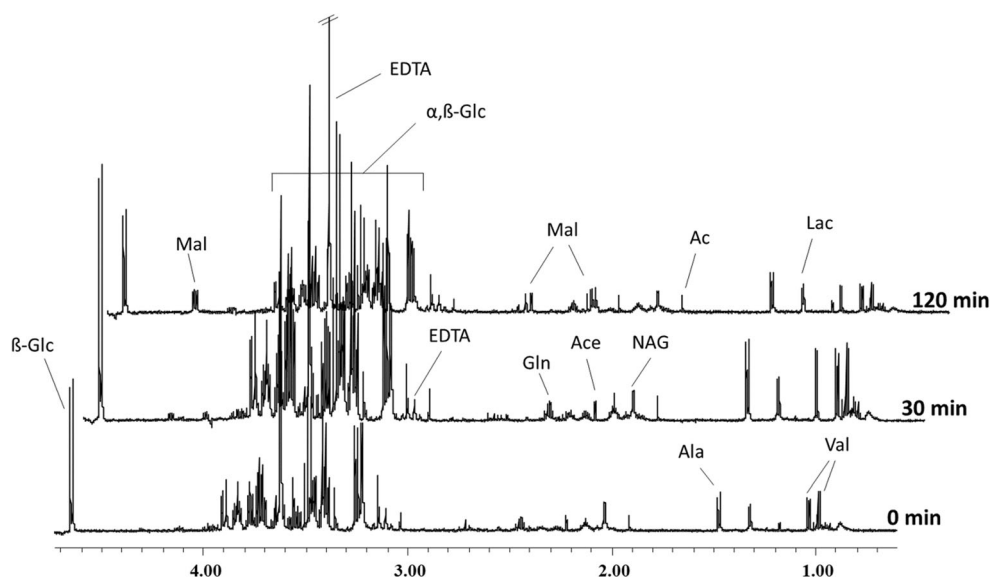
Table 2 Resonance assignment in the ^{1}H-NMR spectra of plasma

|	Compound	δ ^{1}H ppm (multiplicity, assignment)
1	Acetate[a]	1.91 (s, αCH$_3$)
2	Acetoacetate	2.22 (s, CH$_3$)
3	Alanine	1.46 (d, βCH$_3$), 3.77 (t, αCH)
4	Citrate	2.51 (d, α,γCH), 2.63 (d, α',γ'CH)
5	Creatine	3.01 (s, CH$_3$), 3.91 (s, CH$_2$)
6	Formate	8.46 (s, CH)
7	Glucose	3.22 (m, βC2H), 3.38 (m, αC4H, βC4H), 3.46 (m, βC3,5H), 3.51 (m, αC2H), 3.72 (m, αC3H, βC6H), 3.85 (m, αC5,6H, βC6H), 4.62 (d, βC1H), 5.21 (d, αC1H)
8	Glutamine	2.11 (m, βCH$_2$), 2.43 (m, γCH$_2$), 3.75 (m, αCH)
9	Glycine	3.54 (s, CH$_2$)
10	Isoleucine	0.91 (t, δCH$_3$), 0.98 (d, β'CH$_3$), 1.22 (m, γCH), 1.44 (m, γ'CH), 1.96 (m, βCH), 3.64 (m, αCH)
11	Lactate	1.32 (d, βCH$_3$), 4.12 (q, αCH)
12	Leucine	0.96 (t, δCH$_3$), 1.73 (m, $\beta\gamma$CH$_2$), 3.73 (m, αCH)
13	malic acid	2.34 (dd, C3H), 2.64 (dd, C3H), 4.28 (dd, C2H)
14	*N*-Acetyl glycoproteins	2.01 (s, CH$_3$)
15	Proline	1.99 (m, γCH$_2$), 2.06 (m, β'CH), 3.32 (m, βCH, δ'CH$_2$), 3.4 (m, δCH$_2$), 4.1 (m, αCH)
16	Propylene glycol	1.13 (d, CH$_3$), 3.42 (m, C1H), 3.51 (m, C1H), 3.85 (m, C2H)
17	Serine	3.96 (m, βCH$_2$), 3.85 (m, αCH)
18	Valine	0.96 (d, γCH$_3$), 1.02 (d, γ'CH$_3$), 2.25 (m, βCH), 3.62 (m, αCH)

s singlet, *d* doublet, *dd* doublet of doublets, *t* triplet, *m* multiplet

[a] All metabolites are putatively annotated (level 2 of identification according to Chemical Analysis Working Group (CAWG) Metabolomics Standards Initiative recommendations)

were overlapping to such extent that integration was not possible (Thr, Glu) (Fig. 5). For all the metabolites analyzed, total and incremental areas under the curve were similar in both BPL groups. Furthermore, total amino acid measurements indicate that fasting amino acid concentrations between the two BPL groups are the same. Also, total amino acid content during the experiment did not change (Fig. 6).

Discussion

Global metabolomics analysis of biofluids can provide valuable information on a wide range of physiological processes. Plasma metabolic profiles can be influenced by several factors, spanning from genetics to behavioral and environmental, including food intake, gut-microbiota metabolism, and absorption of specific nutrients [28–30]. The RYGB induces
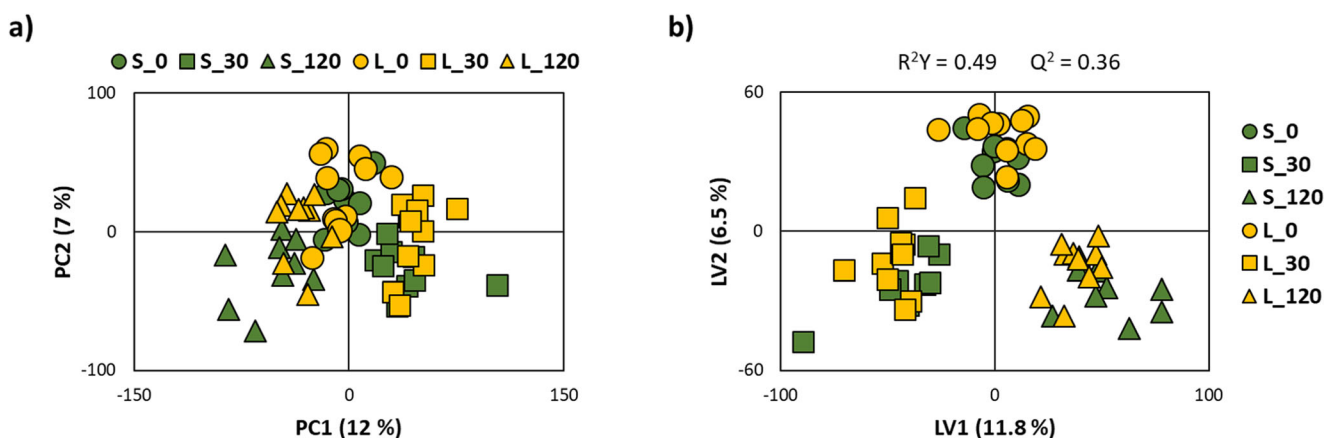
Fig. 2 Score scatterplots resulting from **a** PCA and **b** PLS-DA models of ^{1}H cpmg NMR spectra of plasma of standard (S) and long (L) BPL RYGB at different time points (0, 30, and 120 min) after the oral mixed meal tolerance test
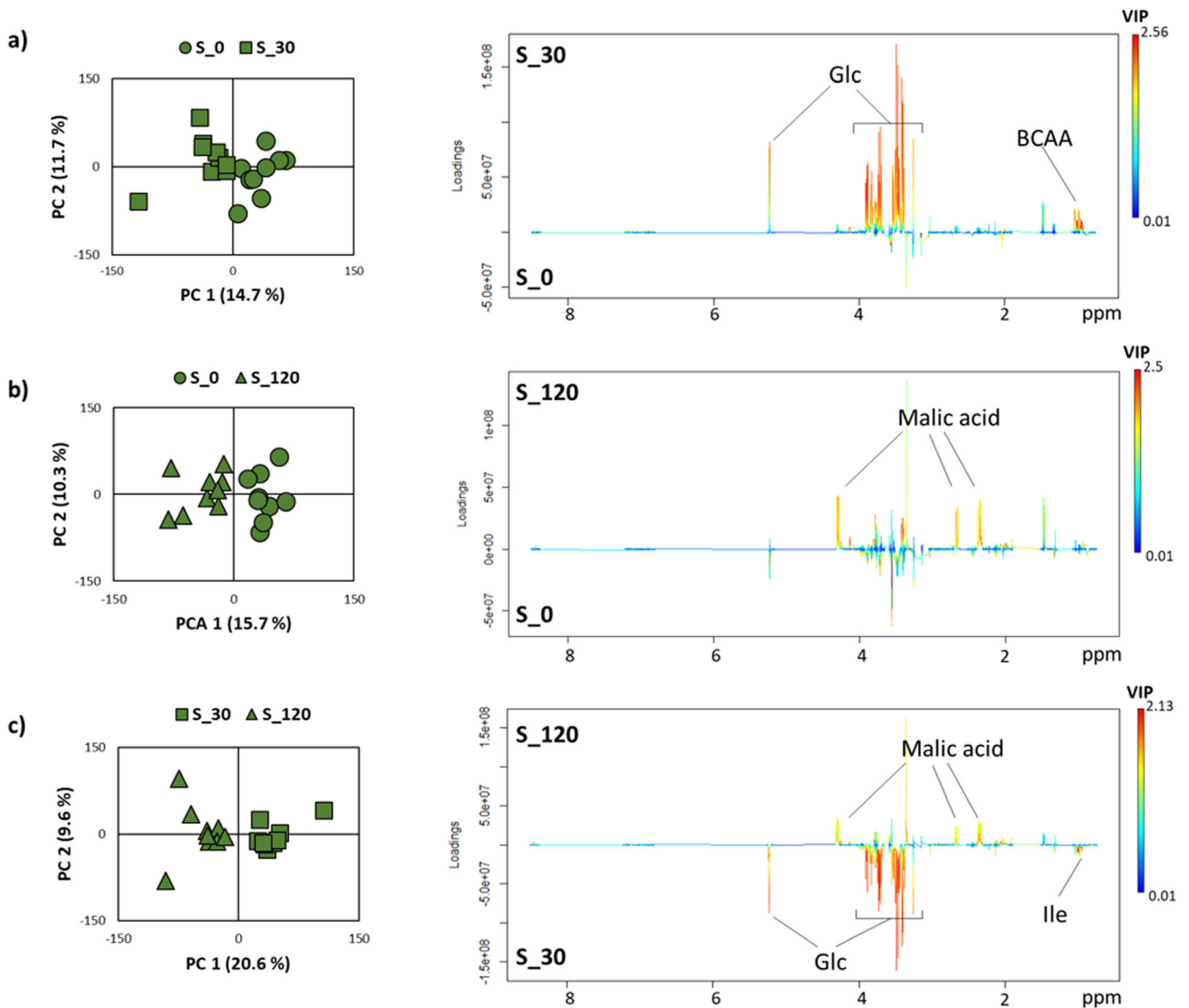
Fig. 3 PCA score plots (left) and corresponding loading plots (right) obtained for cpmg spectra of blood plasma after MMTT for standard BPL. **a** $t = 0$ vs $t = 30$ min post-prandial (S0 vs S30). **b** $t = 0$ vs $t = 120$ min post-prandial (S0 vs S120). **c** $t = 30$ vs $t = 120$ min (S30 vs S120) post-prandial. Loadings are colored according to variable importance on projection (VIP) and some assignments are indicated: BCAA branched-chain amino acids, Glc glucose

an anatomical rearrangement of the gastro-intestinal tract that modifies several of the abovementioned factors and therefore could potentially result in altered metabolic profiles [31]. Previous studies found that RYGB induces an improvement of plasma metabolic profiles, with early reduction in branched-chain amino acids (BCAAs) and short-chain triglycerides [32, 33]. Extensive evidence has shown that elevated levels of BCAAs and short-chain triglycerides are associated with insulin resistance and T2DM. BCAAs seem to act as a downstream molecular mediator on the pathway to overt T2DM, acting as a biomarker tool for T2D prediction [34, 35]. Besides, since some of the metabolic changes were

observed to precede weight loss, these alterations could not to be exclusively attributed to the weight reduction [33].

Aiming to enhance the anti-diabetic properties of the classically described procedure, a RYGB variant with a 2-m-long BPL was introduced by our surgical team [4, 17]. This technical variant was demonstrated to have additional clinical benefits in the outcomes of patients with T2D when compared to the standard intervention, without increasing the risks of surgical or medical complications, including nutrient deficiencies [4, 17, 36]. Nevertheless, modifying the anatomy of the small gut inevitably leads to an additional reduction of the absorptive intestinal surface as compared to the
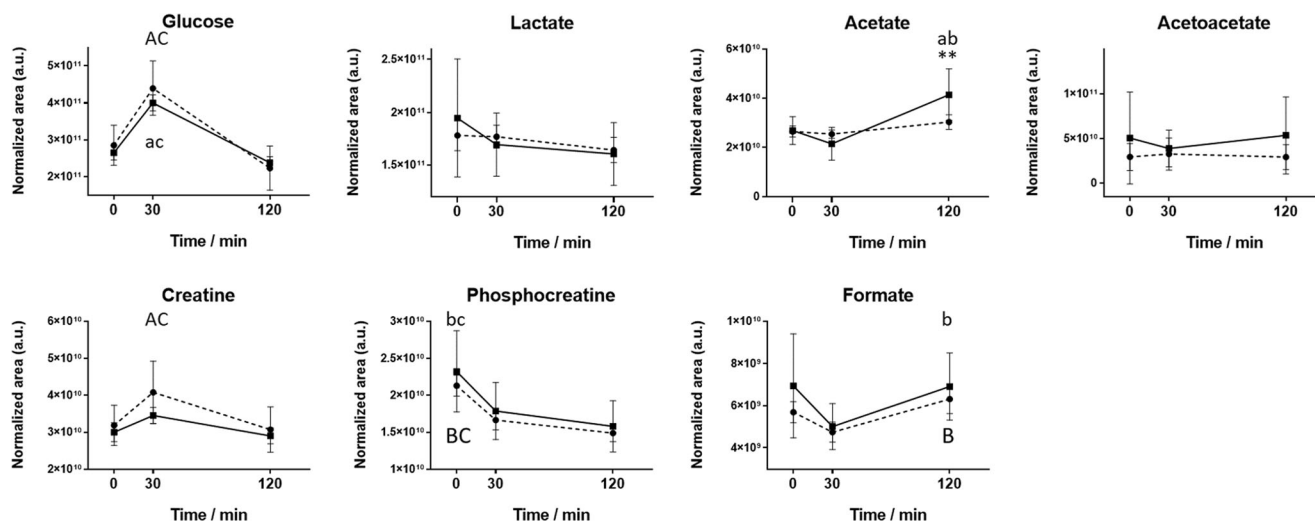
Fig. 4 Changes in miscellaneous metabolites. Results are expressed as mean ± SEM (peak areas normalized by total peak area, a.u.). Results were tested by two-way ANOVA with respective multicomparison correction and were considered significant when $p < 0.05$. Statistical significances of multiple comparisons were marked by the following letter code: each time point group was assigned a letter (0 min = a; 30 min = b; 120 min = c). Uppercase letters indicate difference between standard BPL time points, and lowercase letters between long BP. Differences between standard BPL (dotted line) and long BPL (solid line) were determined by two-tailed t test and are denoted by * (* < 0.05, ** < 0.01)

standard RYGB procedure, thus raising reasonable clinical concerns on the potential negative impact on nutrient absorption profiles.

In order to assess whether a 2-m-long BLP RYGB influences post-absorptive metabolite profiles as compared to the standard intervention, we decided to evaluate and compare the fasting and post-prandial metabolic profiles of subjects submitted to both interventions by the same surgical team, using an ^{1}H-NMR metabolomics approach.

This study shows that in both groups of subjects submitted to RYGB, fasting and post-prandial plasma metabolic profiles are clearly separated. Moreover, since a complete overlap was observed at both time points (0 and 30 min) indicating no difference between metabolite profiles (neither in metabolite species nor concentrations) between the two RYGB procedures, post-prandial plasma metabolomics profiles also suggest that a 2-m-long BLP RYGB does not have a negative impact in acute metabolite absorption. In addition, despite the study included only a small number of subjects that could be a limitation, the reduced variability of the results within each group is reassuring.

In a previous study that compared the metabolic profiles of subjects submitted to RYGB with two different BPL lengths (60 cm vs 60–100 cm), some short-term differences in serum metabolites were found, such as in creatine and in dimethyl sulfone levels [37]. In our current study, creatine levels were also analyzed, but no significant differences between the study groups were identified. The dissimilarities between results of the former and current study could be attributed to the fact that subjects enrolled in our study had a longer post-operative time (RYGB with a shorter BPL: 3.8 ± 2.1 years vs RYGB with a

longer BPL: 4.4 ± 1.7 years), as the differences in circulating metabolite levels between the two interventions were reported to decrease 12 months after RYGB [37]. Besides that, our subjects' RYGB BPL lengths were still different when compared to those of the subjects included in the previous study.

Of particular notice, 120 min after the meal intake, acetate levels were found to be significantly higher in the group of subjects submitted to RYGB with a 2-m-long BPL as compared to the group submitted to the standard RYGB procedure. Although no further mechanistic studies were conducted to dissect the reasons for such an observation, a hypothesis can be raised. Subjects submitted to the RYGB with a longer BPL tend to have a shorter small intestinal length for nutrient absorption, while the contact of undigested food components to biliary and pancreatic secretions is also delayed. Therefore, a greater amount of unabsorbed/undigested nutrients is made available for gut microbiota metabolism in the distal intestine, such as the cecum and colon. In response to that, higher levels of short-chain fatty acids produced in the gut, such as acetate, can be absorbed in the later post-prandial period [38, 39]. Interestingly, prior studies also found that higher levels of circulating acetate were associated with reduced food intake and body weight, along with improved glucose homeostasis and insulin sensitivity [40–42]. So, higher post-prandial acetate levels in the patients previously submitted to RYGB with a longer BPL could also be contributing to the additional benefits in the clinical outcomes of patients with T2D previously observed [17, 36]. Acetate was identified to act as a key metabolite in the crosstalk between the gut microbiota and metabolic organs such
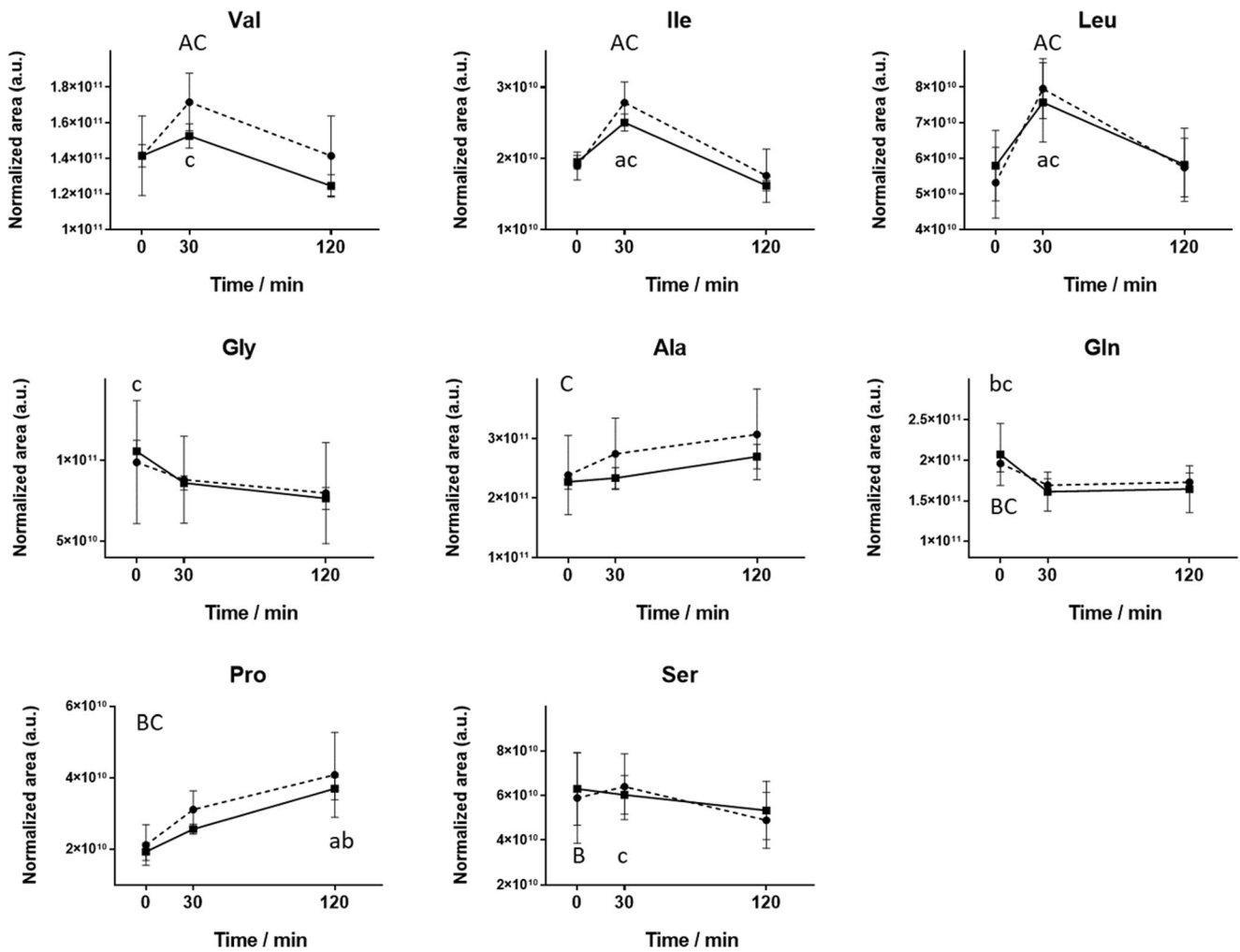
Fig. 5 Changes in amino acid metabolism. Results are expressed as mean ± SEM (peak areas normalized by total peak area, a.u.). Results were tested by two-way ANOVA with respective multiple comparison correction and were considered significant when $p < 0.05$. Statistical significances of multiple comparisons were marked by the following letter code: each time point group was assigned a letter (0 min = a; 30 min = b; 120 min = c). Uppercase letters indicate difference between standard BPL time points, and lowercase letters between long BPL. Differences between standard BPL (dotted line) and long BPL (solid line) were determined by two-tailed t test and are denoted by * (* < 0.05, ** < 0.01)

as liver, adipose tissue, skeletal muscle, brain, and pancreas [38, 43]. Several studies have demonstrated that

acetate triggers several metabolic cascades leading to a decrease in plasma free fatty acid levels, increase in
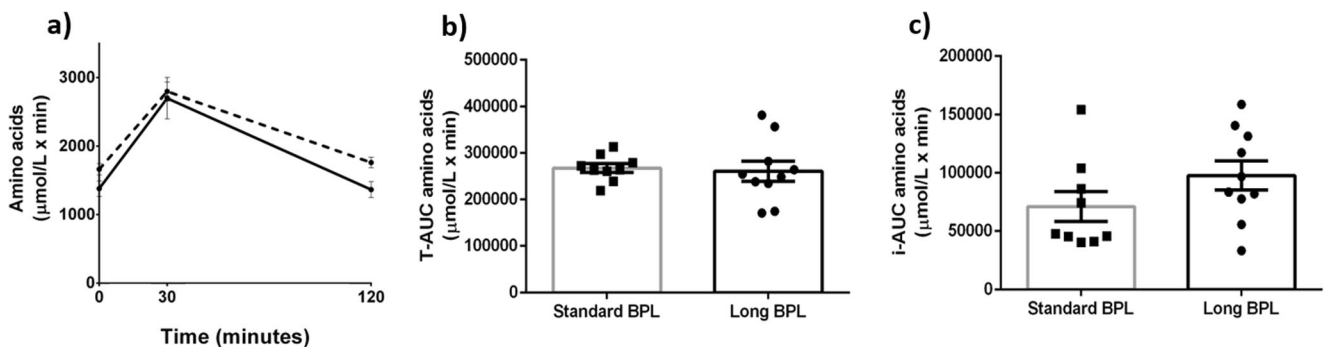
Fig. 6 Plasma levels of amino acids in 20 non-diabetic weight-stable subjects previously submitted to standard RYGB (dotted line) or long BPL RYGB (solid line) after ingestion of a standard mixed meal served at $t = 0$ min and consumed before $t = 15$ min (**a**); total area under the curve (t-AUC) (**b**); incremental area under the curve (iAUC) (**c**). Data are presented as mean values ± SEM

fatty acid oxidation, inhibition of intracellular lipolysis in the adipose tissue, and lipid accumulation in skeletal muscle and liver [44–46]. Acetate was also shown to have a suppressive effect on appetite and energy intake through stimulation of gut-derived satiety hormones, such as GLP-1 and PYY, and via central nervous system-related mechanism [47, 48]. Besides that, acetate is also able to modulate the pro-inflammatory state associated with obesity by increasing the number of anti-inflammatory regulatory T cells and reducing the production of pro-inflammatory cytokines [49–51].

Additionally, subjects submitted to these same two different RYGB procedures were identified to present distinctive post-prandial gastro-intestinal hormone profiles. These endocrine profiles derived from modification of neuro-endocrine cell distribution achieved through different anatomical rearrangements of the small intestine were also hypothesized to contribute for the additional anti-diabetic effects of the modified RYGB with a 2-m-long BPL [17, 18]. However, whether and to which extent nutrient exposure and metabolite absorption contributes for the hormonal secretion profile is still a matter of debate.

Conclusion

These study data suggest that RYGB with a longer BPL does not have a negative impact on acute metabolite transport into circulation. The RYGB BPL length seems to influence post-prandial acetate levels which can potentially contribute for the positive metabolic effects and clinical outcomes of the modified procedure.

Compliance with Ethical Standards

Conflict of Interest The authors declare that they have no conflict of interest.

Ethics All procedures performed in studies involving human participants were in accordance with the ethical standards of the institutional and/or national research committee and with the 1964 Helsinki declaration and its later amendments or comparable ethical standards. Informed consent was obtained from all individual participants included in the study.

References

1. Kizy S, Jahansouz C, Wirth K, et al. Bariatric surgery: a perspective for primary care. Diabetes Spectr. 2017;30(4):265–76.
2. Angrisani L, Santonicola A, Iovino P, et al. Bariatric surgery and endoluminal procedures: IFSO Worldwide Survey 2014. Obes Surg. 2017;27(9):2279–89.
3. Nudel J, Sanchez VM. Surgical management of obesity. Metab Clin Exp. 2019;92:206–16.
4. Nora M, Guimaraes M, Almeida R, et al. Metabolic laparoscopic gastric bypass for obese patients with type 2 diabetes. Obes Surg. 2011;21(11):1643–9.
5. Koliaki C, Liatis S, le Roux CW, et al. The role of bariatric surgery to treat diabetes: current challenges and perspectives. BMC Endocr Disord. 2017;17(1):50.
6. Goldfine AB, Patti ME. Diabetes improvement following Roux-en-Y gastric bypass: understanding dynamic changes in insulin secretion and action. Diabetes. 2014;63(5):1454–6.
7. Maciejewski ML, Arterburn DE, Van Scoyoc L, et al. Bariatric surgery and long-term durability of weight loss. JAMA Surg. 2016;151(11):1046–55.
8. Noria SF, Grantcharov T. Biological effects of bariatric surgery on obesity-related comorbidities. Can J Surg. 2013;56(1):47–57.
9. Jakobsen GS, Smastuen MC, Sandbu R, et al. Association of bariatric surgery vs medical obesity treatment with long-term medical complications and obesity-related comorbidities. Jama. 2018 Jan 16;319(3):291–301.
10. Ionut V, Bergman RN. Mechanisms responsible for excess weight loss after bariatric surgery. J Diabetes Sci Technol. 2011;5(5):1263–82.
11. Rubino F, Forgione A, Cummings DE, et al. The mechanism of diabetes control after gastrointestinal bypass surgery reveals a role of the proximal small intestine in the pathophysiology of type 2 diabetes. Ann Surg. 2006;244(5):741–9.
12. Mingrone G, Castagneto-Gissey L. Mechanisms of early improvement/resolution of type 2 diabetes after bariatric surgery. Diabetes Metab. 2009;35(6 Pt 2):518–23.
13. Svanevik M, Risstad H, Hofso D, et al. Perioperative outcomes of proximal and distal gastric bypass in patients with BMI ranged 50-60 kg/m(2)—a double-blind, randomized controlled trial. Obes Surg. 2015;25(10):1788–95.
14. Nelson WK, Fatima J, Houghton SG, et al. The malabsorptive very, very long limb Roux-en-Y gastric bypass for super obesity: results in 257 patients. Surgery. 2006;140(4):517–22. discussion 22-3
15. Kaska L, Kobiela J, Proczko M, et al. Does the length of the biliary limb influence medium-term laboratory remission of type 2 diabetes mellitus after Roux-en-Y gastric bypass in morbidly obese patients? Wideochirurgia i inne techniki maloinwazyjne = Videosurgery and other miniinvasive techniques. 2014;9(1):31-39.
16. Leifsson BG, Gislason HG. Laparoscopic Roux-en-Y gastric bypass with 2-metre long biliopancreatic limb for morbid obesity: technique and experience with the first 150 patients. Obes Surg. 2005;15(1):35–42.
17. Nora M, Morais T, Almeida R, et al. Should Roux-en-Y gastric bypass biliopancreatic limb length be tailored to achieve improved diabetes outcomes? Medicine (Baltimore). 2017;96(48):e8859.
18. Patricio BG, Morais T, Guimaraes M, et al. Gut hormone release after gastric bypass depends on the length of the biliopancreatic limb. Int J Obes. 2019;43(5):1009–18.
19. Kiela PR, Ghishan FK. Physiology of intestinal absorption and secretion. Best Pract Res Clin Gastroenterol. 2016;30(2):145–59.
20. Goodman BE. Insights into digestion and absorption of major nutrients in humans. Adv Physiol Educ. 2010;34(2):44–53.
21. Wewer Albrechtsen NJ, Junker AE, Christensen M, et al. Hyperglucagonemia correlates with plasma levels of non-

branched-chain amino acids in patients with liver disease independent of type 2 diabetes. Am J Physiol Gastrointest Liver Physiol. 2018;314(1):G91–g6.

22. Wishart DS, Feunang YD, Marcu A, et al. HMDB 4.0: the human metabolome database for 2018. Nucleic Acids Res. 2018;46(D1): D608–d17.

23. Jarak I, Carrola J, Barros AS, et al. From the cover: metabolism modulation in different organs by silver nanoparticles: an NMR metabolomics study of a mouse model. Toxicol Sci. 2017;159(2): 422–35.

24. Savorani F, Tomasi G, Engelsen SB. icoshift: a versatile tool for the rapid alignment of 1D NMR spectra. J Magn Reson. 2010;202(2): 190–202.

25. Dieterle F, Ross A, Schlotterbeck G, et al. Probabilistic quotient normalization as robust method to account for dilution of complex biological mixtures. Application in 1H NMR metabonomics. Anal Chem. 2006;78(13):4281–90.

26. Triba MN, Le Moyec L, Amathieu R, et al. PLS/OPLS models in metabolomics: the impact of permutation of dataset rows on the K-fold cross-validation quality parameters. Mol BioSyst. 2015;11(1): 13–9.

27. Čuperlović-Culf M. NMR metabolomics in cancer research: Elsevier; 2012.

28. Abdul Rahim MBH, Chilloux J, Martinez-Gili L, et al. Diet-induced metabolic changes of the human gut microbiome: importance of short-chain fatty acids, methylamines and indoles. Acta Diabetol. 2019;56(5):493–500.

29. Tebani A, Bekri S. Paving the way to precision nutrition through metabolomics. Front Nutr. 2019;6(41). https://doi.org/10.3389/fnut.2019.00041.

30. Johnson CH, Ivanisevic J, Siuzdak G. Metabolomics: beyond biomarkers and towards mechanisms. Nat Rev Mol Cell Biol. 2016;17(7):451–9.

31. Samczuk P, Ciborowski M, Kretowski A. Application of metabolomics to study effects of bariatric surgery. J Diabetes Res. 2018: 6270875.

32. Arora T, Velagapudi V, Pournaras DJ, et al. Roux-en-Y gastric bypass surgery induces early plasma metabolomic and lipidomic alterations in humans associated with diabetes remission. PLoS One. 2015;10(5):e0126401.

33. Wijayatunga NN, Sams VG, Dawson JA, et al. Roux-en-Y gastric bypass surgery alters serum metabolites and fatty acids in patients with morbid obesity. Diabetes Metab Res Rev. 2018;34(8):e3045.

34. Wang Q, Holmes MV, Davey Smith G, et al. Genetic support for a causal role of insulin resistance on circulating branched-chain amino acids and inflammation. Diabetes Care. 2017 Dec;40(12):1779–86.

35. Wang TJ, Larson MG, Vasan RS, et al. Metabolite profiles and the risk of developing diabetes. Nat Med. 2011 Apr;17(4):448–53.

36. Nora M, Guimaraes M, Almeida R, et al. Excess body mass index loss predicts metabolic syndrome remission after gastric bypass. Diabetol Metab Syndr. 2014 Jan 2;6(1):1.

37. Gralka E, Luchinat C, Tenori L, et al. Metabolomic fingerprint of severe obesity is dynamically affected by bariatric surgery in a procedure-dependent manner. Am J Clin Nutr. 2015 Dec;102(6): 1313–22.

38. Canfora EE, Blaak EE. Acetate: a diet-derived key metabolite in energy metabolism: good or bad in context of obesity and glucose homeostasis? Curr Opin Clin Nutr Metab Care. 2017 Nov;20(6): 477–83.

39. Ríos-Covián D, Ruas-Madiedo P, Margolles A, et al. Intestinal short chain fatty acids and their link with diet and human health. Front Microbiol. 2016;7:185.

40. Perry RJ, Peng L, Barry NA, et al. Acetate mediates a microbiome-brain-beta-cell axis to promote metabolic syndrome. Nature. 2016;534(7606):213–7.

41. den Besten G, van Eunen K, Groen AK, et al. The role of short-chain fatty acids in the interplay between diet, gut microbiota, and host energy metabolism. J Lipid Res. 2013;54(9):2325–40.

42. Lim J, Henry CJ, Haldar S. Vinegar as a functional ingredient to improve postprandial glycemic control—human intervention findings and molecular mechanisms. Mol Nutr Food Res. 2016;60(8): 1837–49.

43. Hernandez MAG, Canfora EE, Jocken JWE, et al. The short-chain fatty acid acetate in body weight control and insulin sensitivity. Nutrients. 2019;18:11(8).

44. Stinkens R, Goossens GH, Jocken JW, et al. Targeting fatty acid metabolism to improve glucose metabolism. Obes Rev. 2015;16(9): 715–57.

45. Fernandes J, Vogt J, Wolever TM. Intravenous acetate elicits a greater free fatty acid rebound in normal than hyperinsulinaemic humans. Eur J Clin Nutr. 2012;66(9):1029–34.

46. van der Beek CM, Canfora EE, Lenaerts K, et al. Distal, not proximal, colonic acetate infusions promote fat oxidation and improve metabolic markers in overweight/obese men. Clin Sci. 2016;130(22):2073–82.

47. Freeland KR, Wolever TM. Acute effects of intravenous and rectal acetate on glucagon-like peptide-1, peptide YY, ghrelin, adiponectin and tumour necrosis factor-alpha. Br J Nutr. 2010;103(3):460–6.

48. Frost G, Sleeth ML, Sahuri-Arisoylu M, et al. The short-chain fatty acid acetate reduces appetite via a central homeostatic mechanism. Nat Commun. 2014;5:3611.

49. Smith PM, Howitt MR, Panikov N, et al. The microbial metabolites, short-chain fatty acids, regulate colonic Treg cell homeostasis. Science. 2013;341(6145):569–73.

50. Soliman ML, Combs CK, Rosenberger TA. Modulation of inflammatory cytokines and mitogen-activated protein kinases by acetate in primary astrocytes. J Neuroimmune Pharmacol. 2013;8(1):287–300.

51. Kobayashi M, Mikami D, Kimura H, et al. Short-chain fatty acids, GPR41 and GPR43 ligands, inhibit TNF-alpha-induced MCP-1 expression by modulating p38 and JNK signaling pathways in human renal cortical epithelial cells. Biochem Biophys Res Commun. 2017;486(2):499–505.

Affiliations

Ivana Jarak[1] · Sofia S. Pereira[2,3,4,5] · Rui A. Carvalho[6] · Pedro F. Oliveira[1,4,7] · Marco G. Alves[1,7] · Marta Guimarães[2,3,8] · Nicolai J. Wewer Albrechtsen[9,10,11] · Jens J. Holst[9,10] · Mário Nora[8] · Mariana P. Monteiro[2,3] (iD)

[1]   Biology and Genetics of Reproduction, Unit for Multidisciplinary Research in Biomedicine (UMIB), University of Porto, Porto, Portugal

[2]   Endocrine, Cardiovascular & Metabolic Research, Unit for Multidisciplinary Research in Biomedicine (UMIB), University of Porto, Porto, Portugal

[3]   Department of Anatomy, Institute of Biomedical Sciences Abel Salazar (ICBAS), University of Porto, Jorge Viterbo Ferreira 228, Building 1.3, 4050-313 Porto, Portugal

[4]   Instituto de Investigação e Inovação em Saúde (I3S), Universidade do Porto, Porto, Portugal

[5]   Institute of Molecular Pathology and Immunology of the University of Porto (IPATIMUP), Porto, Portugal

[6]   Department of Life Sciences, Faculty of Science and Technology (FCTUC), University of Coimbra, Coimbra, Portugal

[7]   Department of Microscopy, Institute of Biomedical Sciences Abel Salazar (ICBAS), University of Porto, Porto, Portugal

[8]   Department of General Surgery, Centro Hospitalar de Entre o Douro e Vouga, Santa Maria da Feira, Portugal

[9]   Department of Biomedical Sciences, Faculty of Health and Medical Sciences, University of Copenhagen, Copenhagen, Denmark

[10]   Novo Nordisk Foundation Center for Protein Research, Faculty of Health and Medical Sciences, University of Copenhagen, 2100 Copenhagen, Denmark

[11]   Department of Clinical Biochemistry, Rigshospitalet, Copenhagen, Denmark